International Journal of Remote Sensing
Vol. 29, No. 20, 20 October 2008, 5767–5784

Modelling spatial-temporal change of Poyang Lake using multitemporal Landsat imagery

FENGMING HUI†‡¶, BING XU‡§, HUABING HUANG‡¶, QIAN YU[#] and PENG GONG*‡¶‖

†International Institute for Earth System Science, Nanjing University, Nanjing 210093, China

‡State Key Laboratory of Remote Sensing Science, jointly sponsored by the Institute of Remote Sensing Applications of Chinese Academy of Sciences and Beijing Normal University, Beijing 100101, China

¶Poyang Lake Ecological Research Station for Environment and Health, Duchang 332600, China

§Department of Geography, University of Utah, Salt Lake City, Utah 84112–9155, USA

[#]Department of Geosciences, University of Massachusetts, Amherst, Massachusetts 01003–9297, USA

‖Division of Ecosystem Science, University of California, Berkeley, California 94720-3114, USA

(*Received 19 December 2006; in final form 5 August 2007*)

Poyang Lake is a seasonal lake, exchanging water with the lower branch of the Yangtze River. During the spring and summer flooding season it inundates a large area while in the winter it shrinks considerably, creating a large tract of marshland for wild migratory birds. A better knowledge of the water coverage duration and the beginning and ending dates for the vast range of marshlands surrounding the lake is important for the measurement, modelling and management of marshland ecosystems. In addition, the abundance of a special type of snail (*Oncomelania hupensis*), the intermediate host of parasite schistosome (*Schistosoma japonicum*) in this region, is also heavily dependent on the water coverage information. However, there is no accurate digital elevation model (DEM) for the lake bottom and the inundated marshland, nor is there sufficient water level information over this area. In this study, we assess the feasibility of the use of multitemporal Landsat images for mapping the spatial-temporal change of Poyang Lake water body and the temporal process of water inundation of marshlands. Eight cloud-free Landsat Thematic Mapper images taken during a period of one year were used in this study. We used the normalized difference water index (NDWI) and the modified normalized difference water index (MNDWI) methods to map water bodies. We then examined the annual spatial-temporal change of the Poyang Lake water body. Finally we attempted to obtain the duration of water inundation of marshlands based on the temporal sequence of water extent determined from the Landsat images. The results showed that although the images can be used to capture the snapshots of water coverage in this area, they are insufficient to provide accurate estimation of the spatial-temporal process of water inundation over the marshlands through linear interpolation.

*Corresponding author. Email: penggong@berkeley.edu

International Journal of Remote Sensing
ISSN 0143-1161 print/ISSN 1366-5901 online
http://www.tandf.co.uk/journals
DOI: 10.1080/01431160802060912

1. Introduction

Wetlands are important natural habitats that must be conserved (Williams 1990). They can protect and improve water quality, serve as habitats for fish and wildlife, store floodwater, assist groundwater recharge and maintain surface water flow during dry periods (Reimold 1994, http://www.wetlands.cn/). Water bodies and marshland areas are two primary components of wetland.

Inundation and water bodies have been mapped using optical and radar imagery in several ways. Classification, visual interpretation and density slicing approaches have been used for water body identification in wetland areas with multiband, multitemporal and multisensor imagery (Frazier and Page 2000, Munyati 2000, Chopra *et al.* 2001, Toyra *et al.* 2001, Dechka *et al.* 2002, Parmuchi *et al.* 2002, Wang *et al.* 2002, Hung and Wu 2005, Jain *et al.* 2005). Several methods of water body recognition with National Oceanic and Atmospheric Administration (NOAA) Advanced Very High Resolution Radiometer (AVHRR) data were suggested including a channel 2 model, a temperature model, a difference and a ratio model between channels 2 and 1 (Sheng *et al.* 2001). In fact, these methods have also been applied to Landsat, Indian Remote Sensing (IRS) and Satellite pour l'Observation de la Terre (SPOT) images (McFeeters 1996, Fraser 1998, Yang *et al.* 1998, Du *et al.* 2001, Yang and Zhou 2001, Rogers and Kearney 2004, Chatterjee *et al.* 2005, Deng *et al.* 2005, Jain *et al.* 2005, Overton 2005, Xu 2005). A water body can be distinguished by these methods to determine its extent and flooding over large areas, though there are obvious disadvantages, such as individual pixel misclassification, mixed pixels, high turbidity or shallow depth and confusion of dark shadow.

Poyang Lake is the largest fresh water lake in China. It is an internationally important habitat for several dozen waterfowl species, among which is the endangered species of Siberia cranes (*Grus leucogeranus*) (http://www.poyanglake.net/index.asp). It is important both ecologically and hydrologically to determine the timing and annual inundation period of the marshland. Such information is directly related to the livability of a snail species (*Oncomelania hupensis*) – the intermediate host of schistosome (*Schistosoma japonicum*) in this region (for relevance of snail to schistosomiasis see Xu *et al.* 2006). Schistosomiasis transmission over the Poyang Lake area is not only a health, but also a political and social issue that has influenced the daily life of over 4.4 million local residents (http://www.jxwst.gov.cn/default.aspx?newsid=1219).

The Chinese government has set up a goal to control schistosomiasis transmission by 2015 (http://www.jxwst.gov.cn/default.aspx?newsid=1219, http://www.gov.cn/zwgk/2005-08/15/content_23039.htm). However, due to the vast area of marshland around Poyang Lake, it is still hard to quantify and map snail distribution over this region. Water inundation is an important factor controlling the spread and reproduction of snails, but quantitative information about water inundation over this area has not been mapped before.

It is a challenge to obtain accurate water inundation information on spatial coverage and beginning and ending time over the marshland of Poyang Lake. One would expect this problem could be solved with a digital elevation model (DEM) for the marshland and the bottom of the lake and water level data observed in a time sequence. Unfortunately there is neither a DEM that is accurate enough nor dense enough water level stations. The water level on the lake is so complicated that the level of water could differ by several metres at the same time from the south to the

north of the lake. An alternative is to use remote sensing to map the water coverage on a daily basis. The spatial resolution of weather satellites that can acquire images on a daily basis is not high enough. However, those satellites with sufficiently high spatial resolution do not have a sufficiently high repeat frequency.

In this study we assess the feasibility of Landsat Thematic Mapper data for mapping the spatial temporal dynamics of water coverage of Poyang Lake. We use existing methods to map the water body from available Landsat TM imagery in an annual time sequence. We then examine the annual spatial-temporal change of the Poyang Lake water body. Finally we attempt to obtain the duration and the beginning and ending dates of water inundation of marshlands based on a linear interpolation of the temporal sequence of water extent determined from the Landsat images.

2. Study area

Poyang Lake is located between 28°22′–29°45′ N and 115°47′–116°45′ E. It lies in the northern part of Jiangxi Province, at the southern bank of the lower reach of the Yangtze River (figure 1). Poyang Lake is divided into two parts by Songmen Mountain. The northern part is primarily a water channel joining the lake with the Yangtze River; the southern part contains the primary water body of the lake surrounded by most marshlands. The basin has an average annual temperature of 17°C, annual rainfall ranging from 1400 mm to 1900 mm, and 240–330 days frost-free (Zhang 1988, http://www.poyanglake.net/index.asp). It is 173 km long from

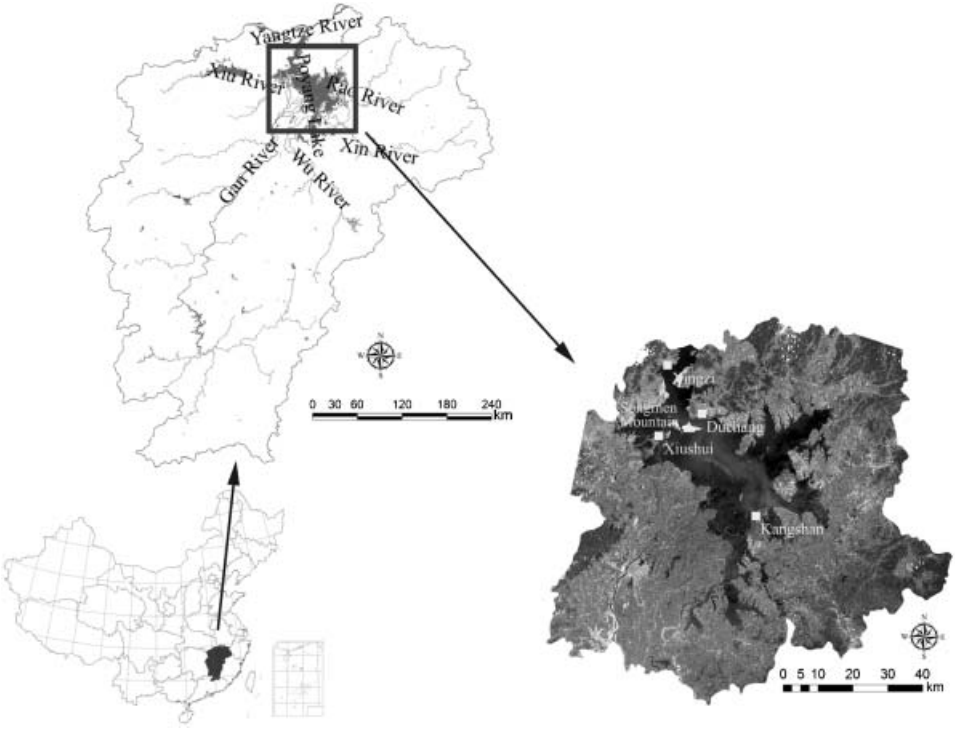

Figure 1. The study area and location of Poyang Lake in China.

north to south. Its furthest width is 74 km, and the mean width is 16.9 km from west to east. The lakeshore is 1200 km long and covers a water area of 3283 km^2 (when the water level at Hukou is 21.71 m, http://www.poyanglake.net/index.asp). Five rivers drain through Poyang Lake (figure 1) into the Yangtze River through Hukou (http://www.poyanglake.net/index.asp). Between April and June, precipitation is concentrated. The lake fills up much like a bathtub, covering all its bottom marshlands, with water from the five rivers. During July to September, water levels in the lake reach a peak with back flowing of water from the Yangtze River. In October and November, the water surface of Poyang Lake subsides. Vast tracts of flat grass-covered marshlands come out of the water. The lake loses as much as 90% of its water. The water body area varies greatly with the fluctuation of its water level. This forms a special scenery of 'marshlands in winter and flood in summer' over the lake area (http://www.poyanglake.net/index.asp).

As an internationally important wetland, it serves important ecological functions. It is also one of the 10 ecological conservation areas in China, and the largest bird conservation area and habitat for migratory birds in the world because of its suitable environment and climatic conditions for migratory birds in winter. More than 98% of the endangered population of Siberia cranes (*Grus leucogeranus)* in the world was found to use the lake area as their winter habitat (http://www.poyanglake.net/index.asp).

3. Image data and preprocessing

3.1 *Image data*

Eight Landsat images, each covering almost the entire Poyang Lake, are selected for mapping the water body dynamics (table 1). They were acquired November 1999 to October 2000 covering both the high and low water level periods. There are small percentages of cloud on six of the images, but all are less than 2%. Among the six images only two have cloud cover over the water areas of Poyang Lake (table 1). Cloud influence is minimal on water body extraction in this study.

In this paper, we focus on the southern section. The Landsat ETM+ image, acquired on 5 July 2000 over the study area, is shown in figure 1.

Table 1. Image data used for water body change in Poyang Lake Basin (GCP, ground control point).

Image date	Landsat sensor	Band list	Correction level*	Cloud/over Poyang Lake	GCP	RMSE (unit: pixel)
16 November 1999	TM	1–5,7	1A	yes/no	22	0.32
10 December 1999	ETM+	1–5,7	1B	no/no	–	–
27 January 2000	ETM+	2,3,4	1A	no/no	26	0.42
16 April 2000	ETM+	1–5,7	1A	yes/no	22	0.21
5 July 2000	ETM+	1–5,7	1B	yes/no	–	–
22 August 2000	ETM+	1–5,7	1A	yes/yes	21	0.36
23 September 2000	ETM+	1–5,7	1B	yes/yes	–	–
9 October 2000	ETM+	1–5,7	1A	yes/no	20	0.33

*Level 1A data product represents radiometrically calibrated data without geometric correction; level 1B data product indicates that data are both radiometrically calibrated and geometric corrected precisely.

3.2 *Radiometric and geometric correction*

Digital number (DN) values acquired from different dates should be converted to apparent surface reflectance to eliminate radiometric differences and remove solar angle differences. Accurate spatial registration of multitemporal images is essential for change detection (Gong *et al.* 1992). Misregistration of two images may result in spurious areas of change being detected from images of different dates. It has been suggested that a root mean squared error (RMSE) of 0.5 pixels is the maximum tolerable error for change detection (Gong and Xu 2003, Jensen 2004).

In this study, all image data were acquired by the Landsat satellites. Seven images were obtained by the Landsat ETM+ onboard Landsat 7 and one was obtained by the Landsat TM onboard Landsat 5. Landsat TM and Landsat ETM+ have almost the same near nadir look angle, and all eight images have the same path and row. The solar angle difference is not removed. We have no information on the atmospheric conditions (e.g. water vapour, aerosol) for each date. We only converted digital number values to apparent reflectance (Chander and Markham 2003, http://landsat.usgs.gov/technical_details/calibration_files/l5_cal_notices/, http://ltpwww.gsfc.nasa.gov/IAS/handbook/handbook_htmls/chapter11/chapter11.html) and then normalized the reflectance by the solar zenith angle to remove the solar angle effect. Since we will extract the water body from each individual image, this processing is sufficient and it is unnecessary to derive absolute surface reflectance.

Three of the images have already been geometrically corrected by the data distributor. We checked their geometric accuracy by selecting airports, dams, cross section of roads and bridges as check points. The image of 5 July 2000 was used as the reference image with the two remaining images compared against the reference by calculating coordinate errors between the corresponding check points. Results show that the root mean squared errors (RMSEs) were 0.05 pixels and 0.04 pixels for the images of 10 December 1999 and 23 September 2000, respectively. So the three images could be viewed as geometrically identical. However, the remaining five images were not geometrically corrected. We selected two images as the master images to geometrically correct the five uncorrected images. Image-to-image registration was performed: the images dated 11 November 1999, 27 January 2000 and 16 April 2000 were registered to the image dated 10 December 1999; the images dated on 22 August 2000 and 9 October 2000 were registered to the image dated on 23 September 2000. All were registered using first order polynomials. RMSEs for all images are listed in table 1, which shows satisfactory registration results.

4. Water body detection

The spectral characteristics of water are remarkably different from other surface types (e.g. vegetation, soil, rock) because of their strong absorption. Clear water has a low spectral reflectance ($<10\%$) in the visible spectral region while other surface covers have higher reflectance than water. However, the reflectance of water increases and peaks at longer wavelengths when mud and sand are in the water. The increase stops when the peak of the water reflectance is located around 0.8 μm (Chen and Zhao 1990, Zheng and Chen 1995).

Methods for differentiating a water body from other surface types have been studied by many researchers (McFeeters 1996, Frazier and Page 2000, Munyati 2000, Chopra *et al.* 2001, Sheng *et al.* 2001, Toyra *et al.* 2001, Dechka *et al.* 2002,

Parmuchi *et al.* 2002, Wang *et al.* 2002, Huang and Wu 2005, Jain *et al.* 2005, Xu 2005). Density slicing and threshold approaches are easy and valid methods for identifying water body. It has been suggested that density slicing approaches and simple thresholds in bands 4, 5 and 7 of Landsat data could give good estimations of water body but might include lots of non-water pixels when compared with aerial photography and results derived from DEMs (Frazier and Page 2000, Jain *et al.* 2005). The normalized difference water index (NDWI) produced the best results for delineating flood-prone areas compared with the density slicing approach using different bands and the Tasselled Cap transformation (Jain *et al.* 2005).

Here we choose a simple but effective band ratio method called the modified NDWI (MNDWI) (Xu 2005) to identify water body. MNDWI was the further development of NDWI (McFeeters 1996). They are defined in the following:

$$NDWI = [\rho_{0.56} - \rho_{0.83}]/[(\rho_{0.56} + \rho_{0.83}] \quad (1)$$

$$MNDWI = [\rho_{0.56} - \rho_{1.65}]/[\rho_{0.56} + \rho_{1.65}] \quad (2)$$

Where $\rho_{0.56}$ is the apparent reflectance at 0.56 μm, $\rho_{0.83}$ is the apparent reflectance at 0.83 μm, $\rho_{1.65}$ is the apparent reflectance at 1.65 μm. $\rho_{0.56}$, $\rho_{0.83}$ and $\rho_{1.65}$ correspond to TM bands 2, 4 and 5, respectively.

The NDWI was developed primarily to delineate water bodies and enhance its presence in remotely sensed imagery while simultaneously eliminating soil and vegetation features (McFeeters 1996). MNDWI can reveal subtle features of water more efficiently than NDWI or the use of other visible spectral bands. It can also remove shadow effects on water, which are otherwise difficult to remove (Xu 2005).

However, the image acquired on 27 January 2000 contains only three bands (bands 2, 3 and 4). With this image it is impossible to use MNDWI. Instead, NDWI and negative normalized difference vegetation index (NDVI multiplied by –1) were calculated together. The remaining seven images allowed for MNDWI calculations. It is impossible to use only one MNDWI value for all images to identify water body. 'Red edge shift' will possibly appear because of different contents of mud and sand at different times over the water body of Poyang Lake. We selected sample points and calculated MNDWI (except the one with NDWI and negative NDVI). Table 2 lists the range and average of MNDWI (or NDWI/negative NDVI) for water, bare land, residential areas, vegetation and cloud. The smallest number of samples among all types was 22 pixels and the greatest was 49 pixels. Bare land includes cropland after harvest; residential area refers to urban and village; vegetation indicates forest, grass and crops. There are two images with cloud calculation because cloud is over water body in those two images.

It can be easily found that the average MNDWI of water is much higher than other cover types in each image, and at the same time the minimum MNDWI value of water is also considerably higher than the maximum MNDWI value of other cover types except for clouds. Therefore, we set a threshold value for each image according to table 2. NDWI and negative NDVI for the image acquired on 27 January 2000 are compared because of the shortage in image bands. There is a sharp contrast in the negative NDVI for water and other surface cover types when compared with the NDWI image. The minimum negative NDVI value of water samples is 0.276, so the threshold should be a little less than 0.276, thus 0.25 was chosen as the threshold value for water extraction with the negative NDVI image. It is impossible to remove all the influences of clouds because of their different

Table 2. Ranges and averages of MNDWI (NDWI/negative NDVI) for each surface type.

Date	Water		Bare land		Residential area		Vegetation		Cloud		Threshold value for extraction
	Range	Average	Range	Average	Range	Average	Range	Average	Range	Average	
16 November 1999	0.500–0.702	0.618	−0.446–0.296	−0.395	−0.186–0.056	−0.096	−0.466–0.178	−0.379	–	–	0.4
10 December 1999	0.514–0.850	0.655	−0.168–0.041	−0.101	−0.076–0.376	0.166	−0.223–0.049	−0.135	–	–	0.45
16 April 2000	0.708–0.808	0.766	−0.015–0.338	0.012	−0.047–0.278	0.055	−0.253–0.041	−0.192	–	–	0.5
5 July 2000	0.447–0.661	0.562	−0.292–0.104	−0.221	−0.292–0.197	−0.115	−0.267–0.091	−0.183	–	–	0.4
22 August 2000	0.537–0.736	0.658	−0.276–0.182	−0.225	−0.276–0.283	−0.044	−0.220–0.023	−0.108	0.121–0.467	0.29	0.45 and mask
23 September 2000	0.553–0.692	0.627	−0.286–0.098	−0.197	−0.287–0.285	−0.037	−0.141–0.008	−0.04	−0.029–0.457	0.052	0.45 and mask
9 October 2000	0.404–0.667	0.548	−0.271–0.096	−0.23	−0.271–0.248	−0.013	−0.224–0.008	−0.146	–	–	0.35
27 January 2000 NDWI	0.214–0.500	0.367	−0.098–0.026	−0.041	0.107–0.232	0.163	−0.333–0.100	−0.196			
27 January 2000 negative NDVI	0.276–0.473	0.377	−0.056–0.098	0.039	0.109–0.195	0.153	−0.406–0.157	−0.237			0.25

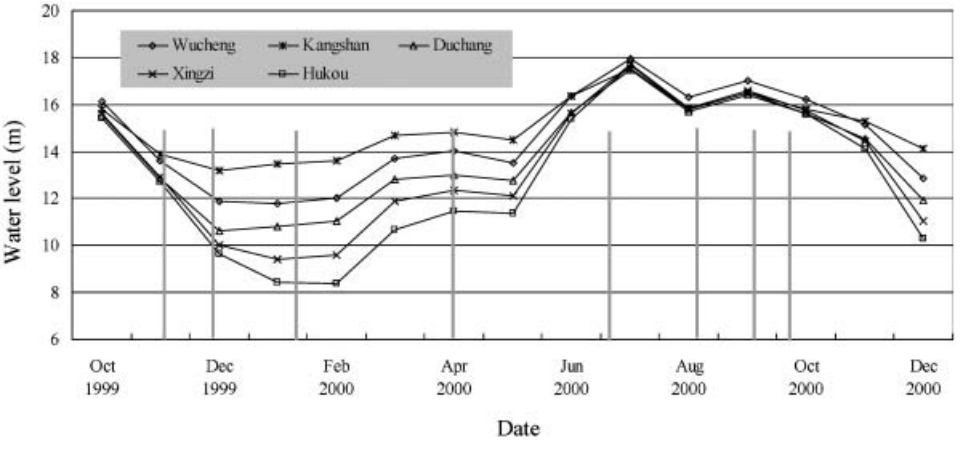

Figure 2. Water level of five hydrological stations from October 1999 to December 2000. Four hydrological stations are marked by squares in figure 1; Hukou is not located in the study area. Grey bar lines indicate the image acquisition dates.

thickness. In order to reduce their influence, we first made a cloud mask then used the mask to exclude the clouds. Despite this, there is some influence from thin clouds. Results show that water bodies are well distinguished though a small amount of noise exists for the images acquired on 22 August 2000 and 23 September 2000.

5. Analysis of the spatial-temporal change of water body

Monthly water level data are taken from five stations but only four of them are in the study region and they are marked by yellow squares in figure 1. The station not covered is Hukou, which is the joining point between the Yangtze River and Poyang Lake. Based on the Shuttle Radar Topography Mission (SRTM) data, the elevations for Wucheng, Kangshan, Duchang, Xingzi and Hukou are approximately 0 m, 3 m, 20 m, 2 m and 3 m, respectively. Figure 2 illustrates water level changes from month to month from October 1999 to December 2000. Although water levels varied greatly annually their change patterns were similar at the five stations.

The identified water body change by Landsat data is correlated with the change of water level at the five hydrological stations (figures 2, 4 and 5). From the results of the image analysis we find that the water level was the lowest at the end of December 1999 or at the beginning of January 2000 and the highest in July 2000. This is in agreement with the water level of the four hydrological stations except Hukou. The area of water body extracted from the image obtained in July 2000 is 3312 km^2. This area includes Poyang Lake, Junshan Lake, and Qinglan Lake, as well as part of the areas of some rivers entering Poyang Lake. During the imaging period, the area of water body shrank from November 1999 to December 1999, expanded from December 1999 to July 2000, and then shrank again from July 2000 to October 2000. The graph of water level (figure 2) resembles that of water body (figure 3) mapped from the eight images. Both can give good descriptions of water variations with time.

In order to examine the spatial-temporal distribution of the water coverage over Poyang Lake, we converted the water boundaries into a shape file. Water coverage of November 1999 and December 1999 were put in one group; those from December

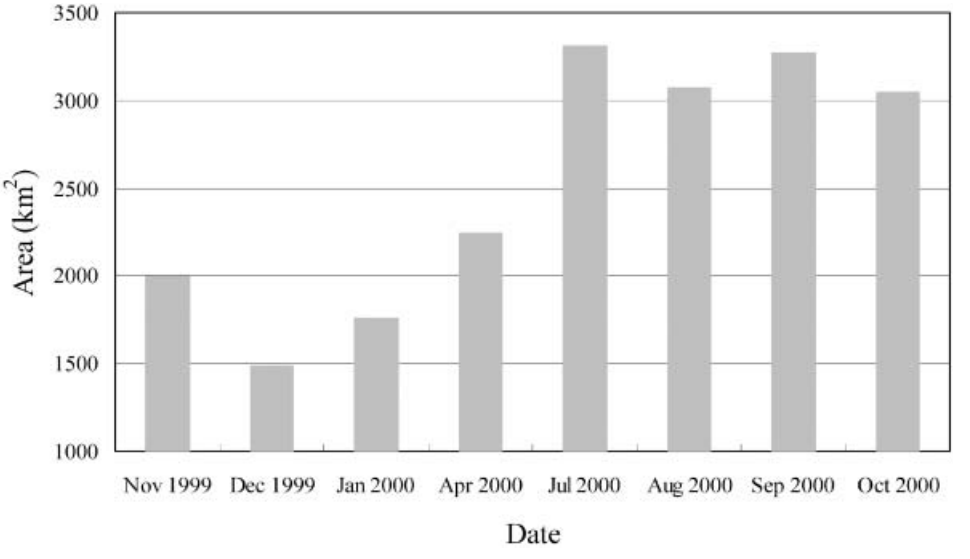

Figure 3. Water body area derived from Landsat data.

1999 to July 2000 were put in the second group and those from July 2000 to October 2000 were put in the third.

In the first group a land area of 515.45 km^2 gradually emerged during a period of 24 days from 16 November 1999 to 10 December 1999. The lake became narrow river channels linking some deep water areas in December 1999. Most marshlands emerged out of the water surface.

In the second group, Poyang Lake has the greatest water body area in July 2000, more than twice the water body area in December 1999. The smallest water body in December 1999 is presented in Sahara sand colour in figure 4 (colour names are from the colour catalogue of ArcGIS software in this paper). In figure 4, the Sahara sand colour represents an area of 1483.26 km^2 covered by water during the entire period of 208 days from December 1999 to July 2000. It is this area that has nearly the lowest water level within a period between November 1999 and October 2000. Therefore, we can infer that the area of 1483.26 km^2 in Sahara sand colour continues to be covered by water for almost the entire year. The medium apple colour represents an area of 404.76 km^2 that gets gradually inundated during a period of 48 days from 10 December 1999 to 27 January 2000; the fuchsia pink colour and the cretean blue colour stands for marshland areas gradually submerged whose sizes are 834.09 km^2 and 1287.40 km^2, respectively. The area in fuchsia pink colour is gradually flooded during a period of 80 days from 27 January 2000 to 16 April 2000 and that of cretean blue colour is gradually covered by water in another period of 80 days from 16 April 2000 to 5 July 2000.

In the third group, the area of water body was reduced from July 2000 to August 2000; while it expanded from August 2000 to September 2000; and then it reduced again from September 2000 to October 2000. Changes are much more complicated than those in the first and the second groups. We have two sub-groups (1) July, August and September 2000 (figure 5(*a*)) and (2) September and October 2000 (figure 5(*b*)). In July 2000 Poyang Lake has the greatest water body area. At that time, most of the marshlands were submerged. The water area is the smallest in

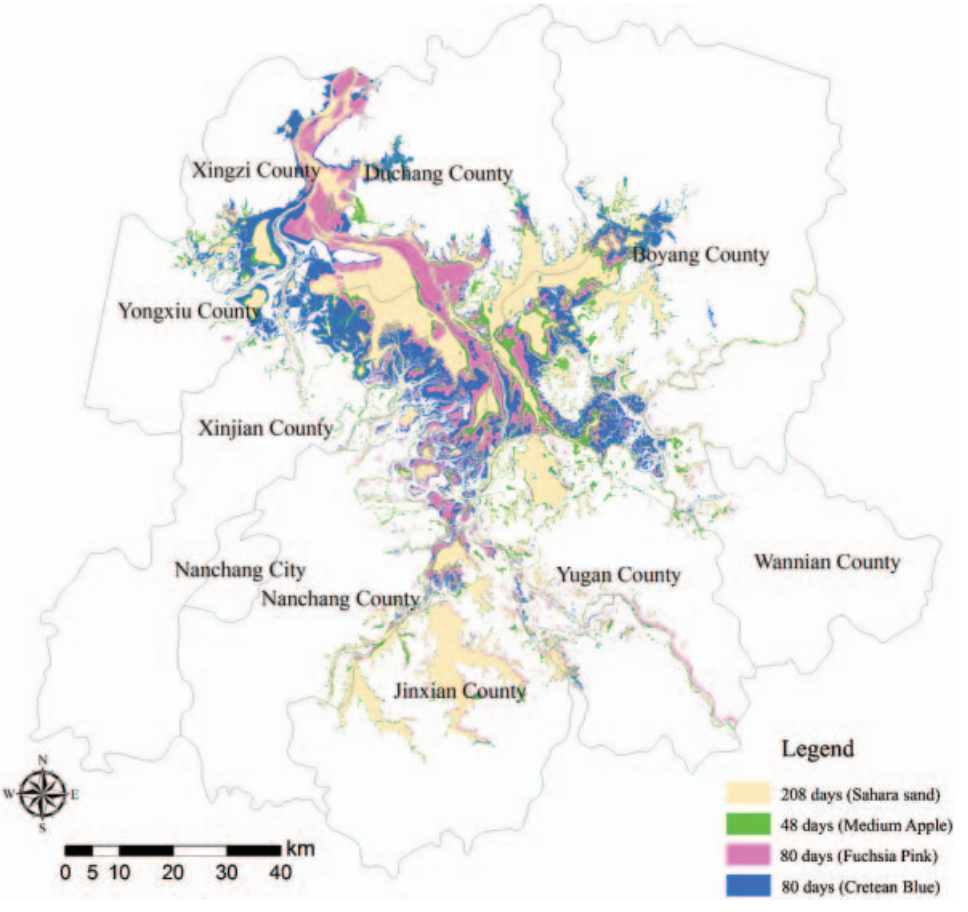

Figure 4. Water body change from December 1999 to July 2000. Number of days represents the duration of water coverage. Colours are taken from the colour catalogue of the ArcGIS software.

October 2000 during the period from July 2000 to October 2000 displayed in Sahara sand colour shown at the bottom of figure 5. The Sahara sand colour represents an area of 3048.04 km^2 covered by water lasting 96 days from July 2000 to October 2000 (it can also be concluded from figures 2 and 3). In figure 5(*a*), the medium apple colour represents the water body area in August 2000, which is the smallest from July to September 2000. The cretean blue colour represents the area gradually emerging out of the water during a period of 48 days from 5 July 2000 to 22 August 2000 and the fuchsia pink colour represents the area gradually flooded during a period of 32 days from 22 August 2000 to 23 September 2000. It can be easily found from figure 5(*a*) that the area flooded from August to September 2000 is mostly areas emerging out of the water from July 2000 to August 2000. These areas are flooded and emerged more than once in a year, mainly influenced by precipitation, water draining into Poyang Lake from the five rivers and change in the water level of the Yangtze River. The increased water area of 249.64 km^2 from 22 August to 23 September (the fuchsia pink colour in figure 5(*a*)) and the reduced area of 250.3 km^2 from 23 September to 9 October (the fuchsia pink colour in figure 5(*b*)) are nearly

the same. So it can be concluded that there is nearly the same water body area in August and October 2000. In fact it is clear in figure 5 that changes in the water body only occur at the edges of Poyang Lake from July to October. The area size of water body during this period in Poyang Lake is closely related to the water level in the Yangtze River at the Hukou station.

During the flood season, river channels are first widened all over the Poyang Lake basin, and then marshlands are gradually inundated by water, and finally marshlands are completely submerged (figure 4). During water retreat, it is exactly the reverse situation: marshlands appear first and then the lake bottom emerges, finally leaving just water channels and deep water areas remaining as standing water (figure 5). Taking the area difference between the smallest and biggest water coverages from December 1999 to July 2000, we obtained an area of 1797.85 km^2 of marshland. Surrounding the lake, Boyang County and Xinjian County contain more than 400 km^2 of marshland, while Yugan County and Duchang County contain more than 250 km^2 of marshland.

6. Mapping the spatial-temporal process of water inundating marshlands

In §5 we are able to capture the snapshots of water coverage during the time of satellite overpass. A general knowledge of marshlands covered by water can be derived from the image analysis results. However, the level of precision is insufficient for determining the number of days of water coverage for each tract of marshland. Such information is needed in studies of marshland growth and snail density distribution. The time length of marshlands under water directly affects wetland productivity, grazing intensity and survival of snails. We attempt to use the water line information extracted in the above section to map the daily spatial pattern of the water inundation process over Poyang Lake and its vicinity.

As described in §5, certain areas will experience multiple times of marshland submerging and emerging. Clearly these up and down trends of water level must be fully captured by the remotely sensed data to derive daily spatial distribution of water coverage. Here we only experiment with the water inundation process and evaluate the potential of our method. It will provide us with more information on the mapping of the temporal process of marshlands under water. Water boundaries obtained from images in December 1999, April 2000 and July 2000 are used for modelling the temporal process of grassland submerging while the water line derived from the January 2000 image is used to validate the temporal modelling.

Temporal modelling is done through a spatial interpolation based on the dates of the waterlines. We interpolate the water line positions on a daily basis between the two dates of known water line positions extracted from the satellite images. The assumptions here are that the water level is rising or falling monotonically in a linear fashion and that between two consecutive dates with satellite derived water line information the water level can only rise or fall, not both. This was achieved by converting the water body boundary of each date into polyline vectors with the date as the attribute, then selecting the boundary polylines under water in two consecutive dates and carrying out an interpolation for this particular period. Here we considered using days only as the attribute. Other factors such as precipitation and water level could have been considered if detailed information on those factors is available. Finally by joining the interpolated days of water polylines during each time period (December 1999–April 2000, April 2000–July 2000) we obtained the total interpolation results (figure 6).

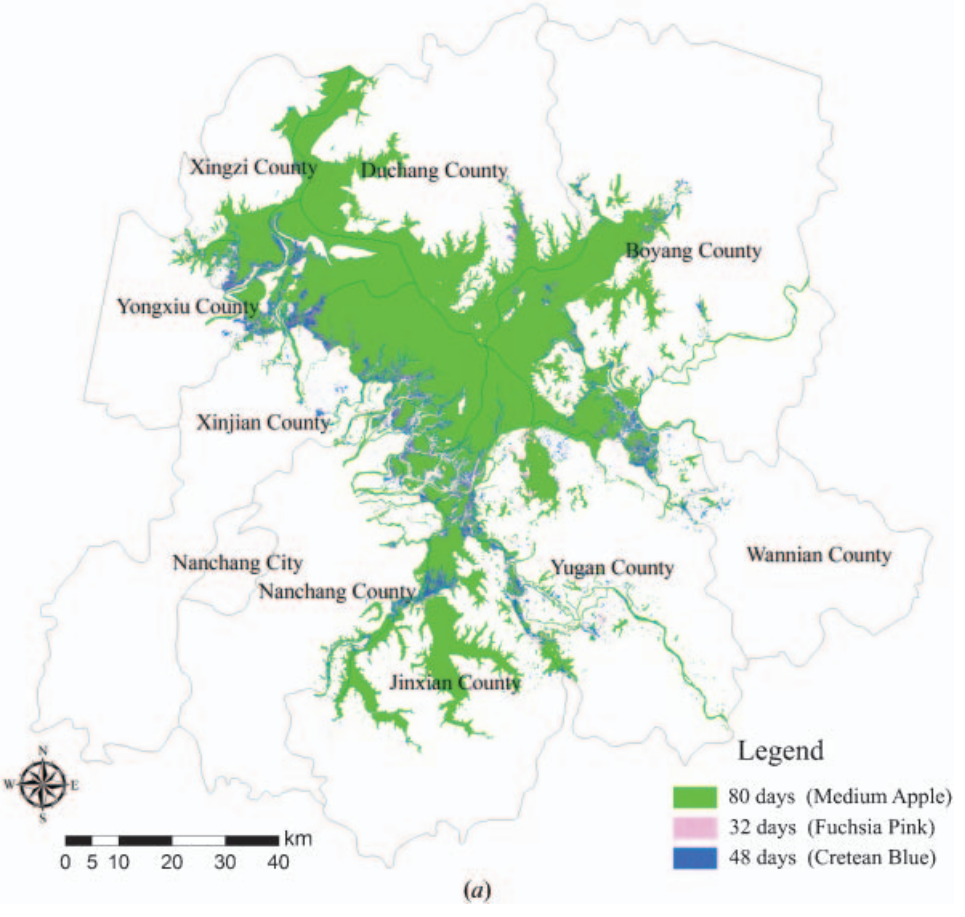

Figure 5. Water body change from July to October 2000. (*a*) Water boundaries in July, August and September 2000. (*b*) Water boundaries in September and October 2000. The number of days represents the duration of water coverage. Colours are taken from the colour catalogue of the ArcGIS software.

With the above method, the water submerging process during any given period can be depicted spatially and temporally. We used the water coverage of January 2000 to validate the interpolation process. We find that the polyline of water boundaries obtained from the 27 January 2000 image runs across the interpolated range from days 10 to 148 (figure 7). In reality, however, it is only 47 days from 10 December 1999 to 27 January 2000. It would be most desirable to see that the interpolated result for day 47 coincided with the actual polyline of the water boundary from the image acquired on 27 January 2000. The interpolated dates for 27 January 2000 vary dramatically in space. By overlaying the water boundary pixels of 27 January 2000 on the interpolation results and producing a histogram of interpolated dates of water submerging marshland (figure 8), we can see that few pixels are around 47. The interpolated results produced only 22.92% of the boundary pixels in the range from 11 January 2000 to 12 February 2000 (the interval of Landsat TM/ETM + image acquired is 16 days). Another test by interpolating the April water boundary has reached similar results. This indicates that there exists a

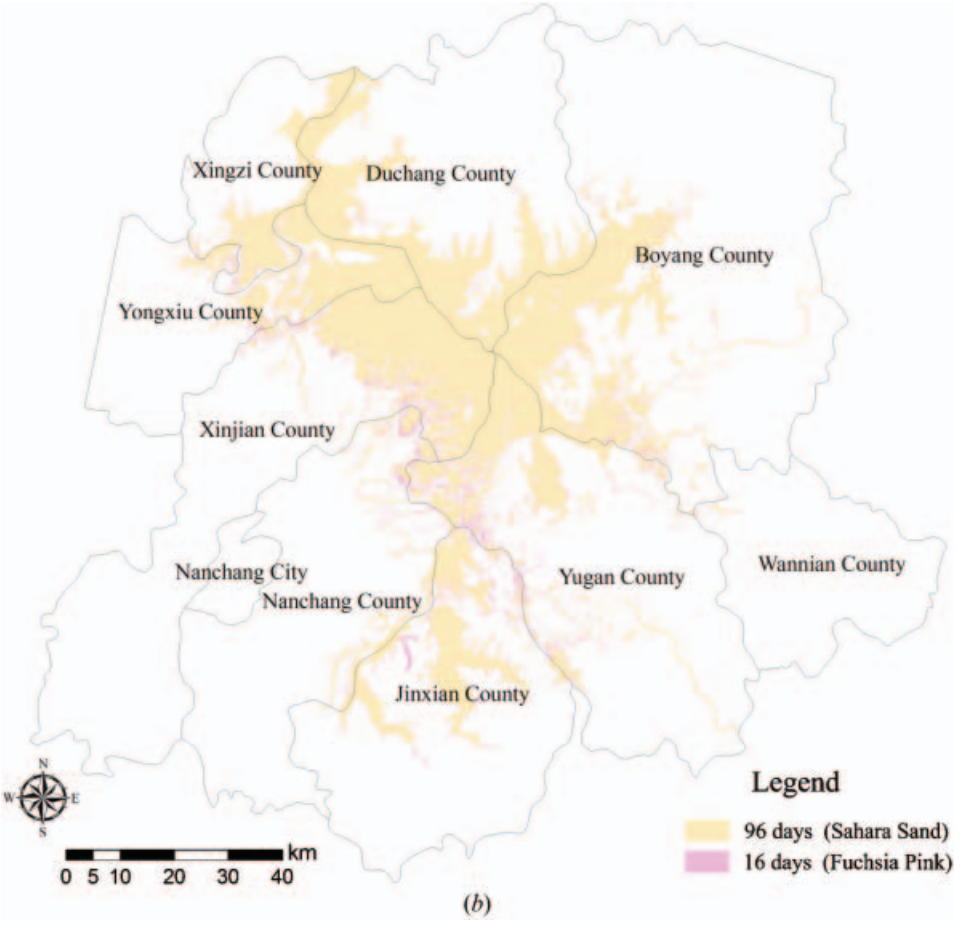

Figure 5. Continued.

large amount of error in the interpolation results. The processes of water submerging and marshland emerging out of water are nonlinear and complex.

7. Discussion

Previous research indicates that water depth or topography of coastal marsh could be derived from flood extent vectors digitized from remotely sensed data combined with lake bottom contours and point measurements of water depth (Prata 1990, Ramsey *et al.* 1998). One would expect that with a DEM or topographic contour map of the lake bottom and daily water level information water coverage should be precisely determined through a water filling procedure. Our experience at Poyang Lake suggests that this cannot be accurately done because the water is rarely level in an open and dynamic system like Poyang Lake. A process model of the spatial temporal dynamics of water coverage over Poyang Lake would require quantitative knowledge of the hydrological processes from all its five tributaries and the Yangtze River at Hukou, water mechanics in the lake and boundary conditions of the lake bottom represented by a DEM. Nonetheless, we have neither a DEM nor a contour

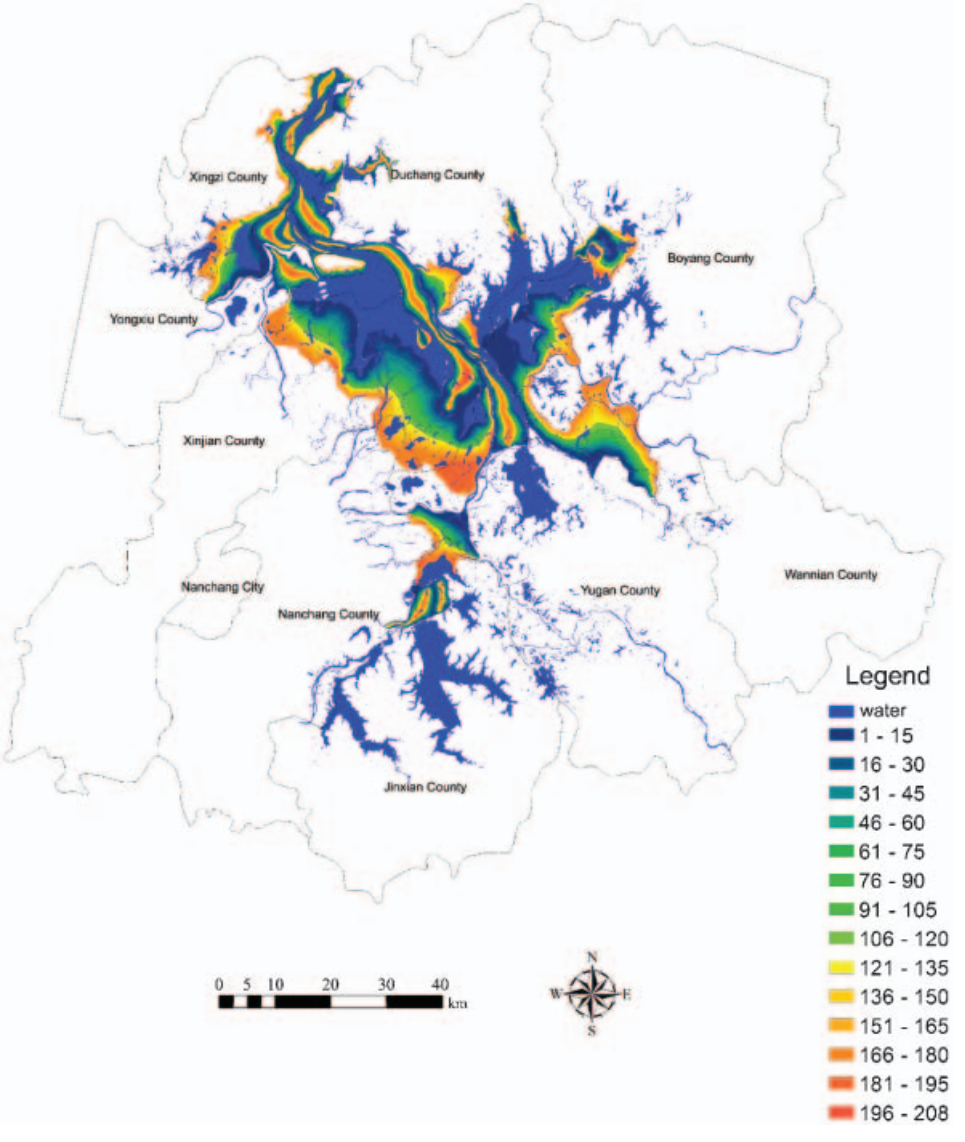

Figure 6. Temporal process of water inundating marshlands from December 1999 to July 2000. The blue colour indicates water cover all year long. The other colours labelled with numbers represent days of marshlands emerging out of water.

map for the lake bottom for Poyang Lake. Therefore, a process-based model for deriving water coverage information is not an option for us at present.

We choose an alternative to mapping the spatial temporal dynamics of water coverage at Poyang Lake based on satellite observation. If daily cloud-free images with acceptable spatial resolution (30 m or better) are available, the method reported in this study would meet our needs. However, qualified daily images are not available at present. Spatial temporal interpolation of existing data is considered as a natural procedure for filling the temporal gaps. Here, our assumption of water expansion or shrinking being linear failed in this assessment. Instead, this process is nonlinear and complex in space. Not only is the precipitation over the Poyang Lake

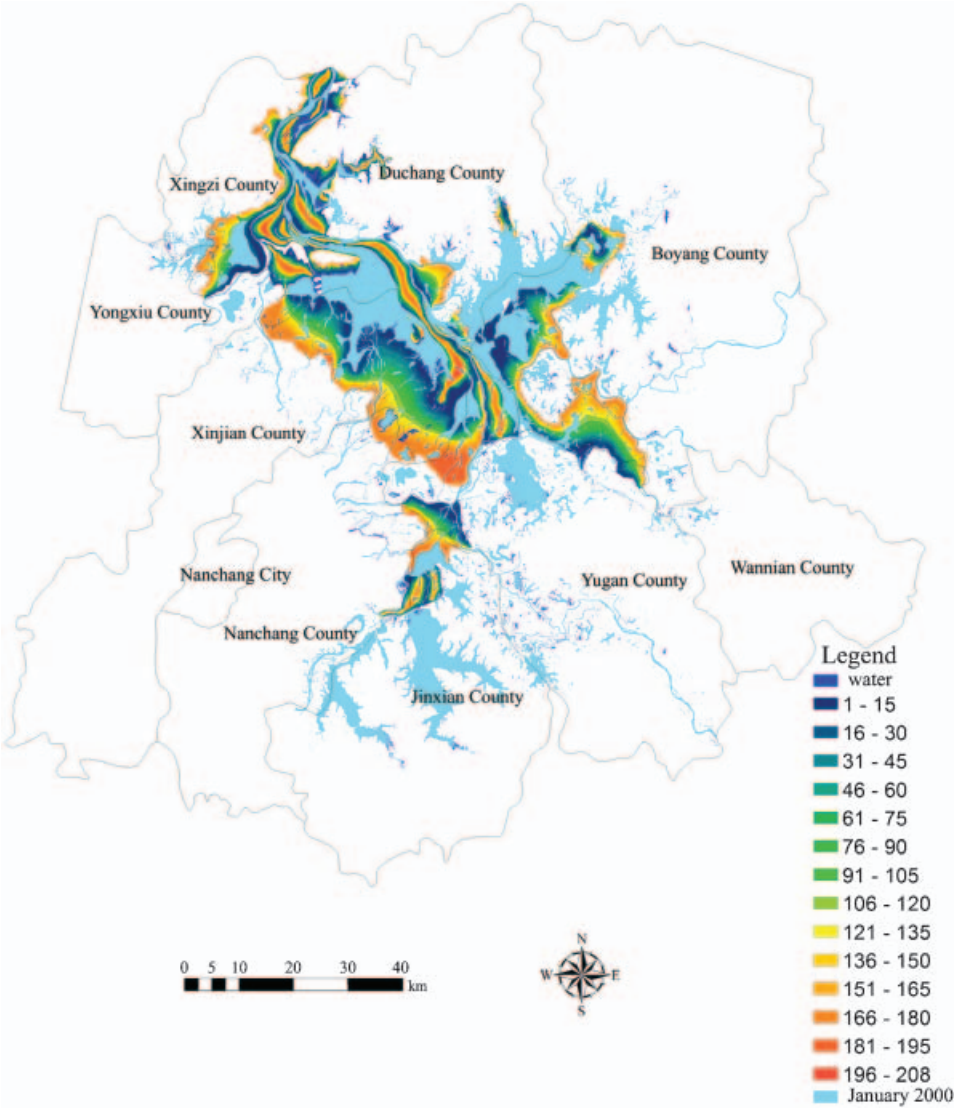

Figure 7. Temporal process of water inundating from December 1999 to July 2000 with water coverage on 27 January 2000. The blue colour indicates water cover all year long. The other colours labelled with numbers represent days of marshlands emerging out of water. The last row stands for the water body coverage on 27 January 2000.

basin and water level rise and fall at the Yangtze River nonlinear, but so is the lake bottom topography. Therefore, nonlinear approaches should be developed. Future work should consider incorporating the sparsely available water level records in the surrounding hydrological stations in a nonlinear interpolation. As a matter of fact, precipitation, water level, micro terrain features, interval of image acquisition may all play a role in the interpolation of water boundaries extracted from multitemporal remotely sensed data.

The interval of two sets of water boundaries has a large impact on the final outcome of the interpolation. The revisit cycle of Landsat 5 or Landsat 7 is 16 days. Because this area is often covered by cloud, it is hard to obtain high temporal

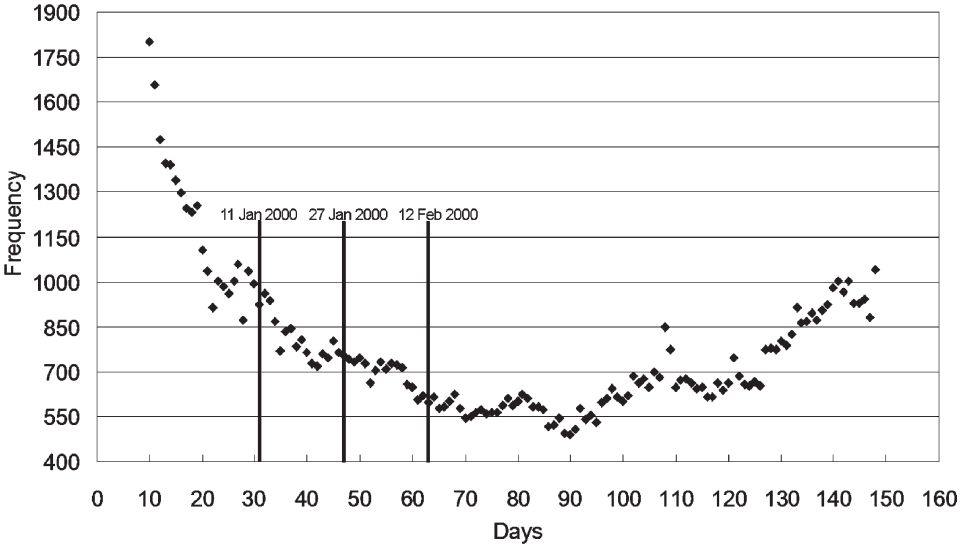

Figure 8. Water boundary pixels derived from the image of 27 January 2000 versus interpolation results at the same boundary pixel locations. *X*-axis is days after 10 December 1999.

frequency of useable Landsat images. A time series of images with a shorter interval is desirable. Presently, only MODIS and NOAA AVHRR could provide daily coverage for the same area. However, their spatial resolutions are coarse. Some kind of unmixing and water boundary determination method must be developed before they could be used for our purpose.

Data from other satellites, particularly cloud-free synthetic aperture radar (SAR) images, should be used for water area extraction. However, they are expensive and their acquisition frequency is not higher.

The ultimate solution to the marshland inundation problem at Poyang Lake would be constructing a model that considers the complex processes of lake filling by upstream rivers and the downstream water inflow, precipitation, wind regime, and complex local variation of topography under the lake bottom. Coupling such a model with water boundary information extracted from remotely sensed data may provide the most accurate information on the spatial temporal dynamics of Poyang Lake.

Acknowledgements

This work was supported by the National Natural Science Foundation of China (grant no. 30590370), the National Scientific Support Project (2006BAJ01B02), the National High Technology Research and Development Program of China (2006AA12Z112) and the K.C. Wong Education Foundation, Hong Kong. We would like to thank Prof. Arthur P. Cracknell from the University of Dundee for his revisions and Dr Lan Mu from the University of Illinois for her suggestions on calculating the temporal process of water inundating marshlands. The comments of two anonymous referees are also appreciated.

References

CHANDER, G. and MARKHAM, B., 2003, Revised Landsat-5 TM radiometric calibration procedures and postcalibration dynamic ranges. *IEEE Transactions on Geoscience and Remote Sensing*, **41**, pp. 2674–2677.

CHATTERJEE, C., KUMAR, R., CHAKRAVORTY, B., LOHANI, A.K. and KUMAR, S., 2005, Integrating remote sensing and GIS techniques with groundwater flow modeling for assessment of waterlogged areas. *Water Resources Management*, **19**, pp. 539–554.

CHEN, S.P., and ZHAO, Y.S. (Ed.), 1990, *Geographic Analysis of Remote Sensing* (in Chinese) (Beijing: SinoMaps Press).

CHOPRA, R., VERMA, V.K. and SHARMA, P.K., 2001, Mapping, monitoring and conservation of Harike wetland ecosystem, Punjab, India, through remote sensing. *International Journal of Remote Sensing*, **22**, pp. 89–98.

DECHKA, J.A., FRANKLIN, S.E., WATMOUGH, M.D., BENNETT, R.P. and INGSTRUP, D.W., 2002, Classification of wetland habitat and vegetation communities using multi-temporal IKONOS imagery in southern Saskatchewan. *Canadian Journal of Remote Sensing*, **28**, pp. 679–685.

DENG, J.S., WANG, K., LI, J. and DONG, Y.Q., 2005, Study on the automatic extraction of water body information from SPOT-5 images using decision tree algorithm. *Journal of Zhejiang University (Agric. & Life Sci.)* (in Chinese), **31**, pp. 171–174.

DU, J.K., HUANG, Y.S., FENG, X.Z. and WANG, Z.L., 2001, Study on water bodies extraction and classification from SPOT image. *Journal of Remote Sensing* (in Chinese), **5**, pp. 214–219.

FRASER, R.N., 1998, Multispectral remote sensing of turbidity among Nebraska Sand Hills lakes. *International Journal of Remote Sensing*, **19**, pp. 3011–3016.

FRAZIER, P.S. and PAGE, K.J., 2000, Water body detection and delineation with Landsat TM data. *Photogrammetric Engineering and Remote Sensing*, **66**, pp. 1461–1467.

GONG, P. and XU, B., 2003, Remote sensing of forests over time: changes types, methods, and opportunities. In *Remote Sensing of Forest Environments: Concepts and Case Studies*, M. Woulder and S.E. Franklin (Eds), pp. 301–333 (Amsterdam: Kluwer Press).

GONG, P., LEDREW E.F. and MILLER, J.R., 1992, Registration noise reduction in difference images for change detection. *International Journal of Remote Sensing*, **13**, pp. 773–779.

HUNG, M.C. and WU, Y.H., 2005, Mapping and visualizing the Great Salt Lake landscape dynamics using multi-temporal satellite images, 1972–1996. *International Journal of Remote Sensing*, **26**, pp. 1815–1834.

JAIN, S.K., SINGH, R.D., JAIN, M.K. and LOHANI, A.K., 2005, Delineation of flood-prone areas using remote sensing techniques. *Water Resources Management*, **19**, pp. 333–347.

JENSEN, J.R. (Ed.), 2004, *Introductory Digital Image Processing: A remote sensing perspective* (3rd edn) (Upper Saddle River, NJ: Prentice Hall).

MCFEETERS, S.K., 1996, The use of the normalized difference water index (NDWI) in the delineation of open water features. *International Journal of Remote Sensing*, **17**, pp. 1425–1432.

MUNYATI, C., 2000, Wetland change detection on the Kafue Flats, Zambia, by classification of a multitemporal remote sensing image dataset. *International Journal of Remote Sensing*, **21**, pp. 1787–1806.

OVERTON, I.C., 2005, Modeling floodplain inundation on a regulated river: integrating GIS, remote sensing and hydrological models. *River Research and Applications*, **21**, pp. 991–1001.

PARMUCHI, M.G., KARSZENBAUM, H. and KANDUS, P., 2002, Mapping wetlands using multi-temporal RADARSAT-1 data and a decision-based classifier. *Canadian Journal of Remote Sensing*, **28**, pp. 175–186.

PRATA, A.J., 1990, Satellite-derived evaporation from Lake Eyre, South Australia. *International Journal of Remote Sensing*, **11**, pp. 2015–2068.

RAMSEY, E.W., NELSON, G.A., LAINE, S.C., KIRKMAN, R.G. and TOPHAMA, W., 1998, Generation of coastal marsh topography with radar and ground-based measurements. *Journal of Coastal Research*, **14**, pp. 1158–1164.

REIMOLD, R.J., 1994, Wetlands functions and values. In *Applied Wetlands Science and Technology*, D.M. Kent (Ed.), pp. 55–78 (London: Lewis Publishers).

ROGERS, A.S. and KEARNEY, M.S., 2004, Reducing signature variability in unmixing coastal marsh Thematic Mapper scenes using spectral indices. *International Journal of Remote Sensing*, **25**, pp. 2317–2335.

SHENG, Y., GONG, P. and XIAO, Q., 2001, Quantitative dynamic flood monitoring with NOAA AVHRR. *International Journal of Remote Sensing*, **22**, pp. 1709–1724.

TOYRA, J., PIETRONIRO, A. and MARTZ, L.W., 2001, Multisensor hydrologic assessment of a freshwater wetland. *Remote Sensing of Environment*, **75**, pp. 162–173.

WANG, Y., COLBY, J.D. and MULCAHY, K.A., 2002, An efficient method for mapping flood extent in a coastal floodplain using Landsat TM and DEM data. *International Journal of Remote Sensing*, **23**, pp. 3681–3696.

WILLIAMS, M., 1990, Protection and retrospection. In *Wetlands: A threatened landscape*, M. Williams (Ed.), pp. 325–353 (Oxford: Blackwell).

YANG, C.J. and ZHOU, C.H., 2001, Application of complementary information of RADARSAT SWA SAR and Landsat TM in deciding the flood extent. *Journal of Natural Disaster* (in Chinese), **10**, pp. 79–83.

YANG, C.J., WEI, Y.M. and CHEN, D.Q., 1998, Investigation on extracting the flood inundated area from JERS-1 SAR data. *Journal of Natural Disaster* (in Chinese), **7**, pp. 45–50.

XU, B., GONG, P., SETO, E., LIANG, S., YANG, C., WEN, S., QIU, D., GU, X.G. and SPEAR, R., 2006, A spatial-temporal model for assessing the effects of inter-village connectivity in schistosomiasis transmission. *Annals of AAG*, **96**, pp. 31–46.

XU, H.Q., 2005, A study on information extraction of water body with the modified normalized difference water index (MNDWI). *Journal of Remote Sensing* (in Chinese), **9**, pp. 589–595.

ZHANG, B. (Ed.), 1988, *Study on Poyang Lake* (in Chinese) (Shanghai: Shanghai Publishing House of Science and Technology).

ZHENG, W., and CHEN, S.P. (Ed.), 1995, *Introduction to Resources Remote Sensing* (in Chinese) (Beijing: Publishing House of Science and Technology).